ON FORECASTING ABNORMAL CLIMATIC EVENTS IN THE TROPICAL ATLANTIC OCEAN

Jacques Servain[1] and Sabine Arnault[2]

March 1995

Final Version

Accepted to be published in

Annales Geophysicae

[1]ORSTOM-UBO, Centre ORSTOM, B.P. 70, 29280 Plouzané, France
[2]LODYC, UMR 121, CNRS/ORSTOM/UPMC, 4 Place Jussieu, 75252 Paris, France

ON FORECASTING ABNORMAL CLIMATIC EVENTS IN THE TROPICAL ATLANTIC OCEAN

Jacques Servain[1] and Sabine Arnault[2]

March 1995

Final Version

Accepted to be published in

Annales Geophysicae

[1]ORSTOM-UBO, Centre ORSTOM, B.P. 70, 29280 Plouzané, France
[2]LODYC, UMR 121, CNRS/ORSTOM/UPMC, 4 Place Jussieu, 75252 Paris, France

ABSTRACT

Modeling and observational evidence indicate that interannual variabilities of dynamic height and sea surface temperature (SST) in the eastern part of the tropical Atlantic Ocean (Gulf of Guinea) are largely induced by preceding fluctuations in wind stress, mainly in the western equatorial basin. A wind-driven linear oceanic model is used here to test the possibility of forecasting the abnormal dynamic heights. A control run of the model, forced by 1964-1993 wind stress monthly means, is first conducted. Yearly test runs (1964-1994) are subsequently performed from January to August by forcing the model with observed winds from January to May, and then by May wind assumed to persist from June to August. During the last three decades the largest deviations of dynamic height simulated by the control run in the Gulf of Guinea in boreal summer would have been correctly forecast from wind data only related to conditions in May of each year. However, for weak climatic anomalies, the model may forecast overestimated values. For the most part (about 20 times during the last 30 years), the sign of observed SST anomaly in the center of the Gulf of Guinea during the boreal summer is identical to the sign of simulated anomalies of dynamic height deduced from both control and test runs. Along the eastern equatorial wave-guide, the sea level forecasting skill slowly decreases from the first fortnight of June until the second fortnight of August, but remains high on both sides of the equator throughout boreal summer, as is expected from the adjustement in a linear oceanic model. It is established that all year long in the Gulf of Guinea, the accuracy of the one-month forecast dynamic height anomaly provided by the simple linear method is greater than that of the one-month forecast assuming the persistence.

INTRODUCTION

Though the climatic variability over the tropical Atlantic Ocean is largely dominated by the seasonal cycle (Philander, 1979; Merle, 1980), the interannual signal is also well marked and has been observed in various *in situ* (*e.g.* Servain *et al.*, 1985) and satellite (*e.g.* Arnault and Cheney, 1994) data sets. However, much more that in the Pacific, tropical Atlantic interannual variability strongly relates in space and time to seasonal changes (Merle *et al.*, 1980; Servain *et al.*, 1985). Consequently, the life-time of abnormal climatic events is relatively short, usually from a few weeks to a few months (Zebiak, 1993), rarely more. The very low-frequency signal (at decadal and longer time-scale), which also appears in the tropical basin (Servain, 1991), probably relates to thermohaline processes involving the whole Atlantic Ocean and will not be discussed here.

Atlantic interannual variability has sometimes been considered as an El Niño-like event (Hisard, 1986). It is generally associated either to droughts or floods in surrounding countries (Hastenrath and Heller, 1977; Moura and Shukla, 1981) and affects pelagic fisheries in the eastern basin (Fonteneau, 1991). However, up to now, no attempt has been made to numerically forecast the largest abnormal climatic events in the tropical Atlantic, contrary to Pacific El Niño events (Inoue and O'Brien, 1984; Cane and Zebiak, 1985; Barnett *et al.*, 1988; Leetmaa and Ji, 1988; Latif and Flugel, 1991). In this paper, we propose a pilot study to forecast the dynamic height anomalies by means of a linear model similar to that used by Inoue and O'Brien (1984) for the equatorial Pacific ocean. In this model the only forcing is the wind stress and sea surface temperature (SST) is not one of the numerical variables. Consequently, we will not numerically forecast the SST. Nevertheless, the numerical model results can be placed in the context of the empirically based relations between remote winds and Gulf of Guinea SST

established in prior work (Servain *et al.*, 1982, 1985) and of which we provide some new elements in the first part of this paper.

The most important season to study interannual variability and undertake a forecast is when variance is strongest. In previous empirical studies of the tropical Atlantic (Servain *et al.*, 1985), it was shown that SST anomalies are greatest in the Gulf of Guinea during boreal summer (June-August), *i.e.*, where and when the thermocline is quite close to the surface and experiences important vertical movements which strongly affect the fertilisation of the euphotic zone. Therefore, the June to August period was selected to test our oceanic forecasting experiment.

After a brief review on the mechanisms driving the tropical Atlantic variability, especially for the Gulf of Guinea, we present the materials (data and model) used in this study. We then focus on the relationship between the anomalies of wind stress, dynamic height and SST during boreal spring and summer. In the third part of the paper, we test a simple dynamic height forecasting experiment for each summer from 1964 to 1994.

THE DYNAMICS OF CLIMATIC VARIABILITY IN THE GULF OF GUINEA

It is widely claimed that the equatorial oceans respond clearly and coherently to large-scale, low-frequency wind fluctuations. However, the nature of the response critically depends on the spatial distribution of the wind field. In the case of the tropical Atlantic, the oceanic response is complex and not yet fully understood (*e.g.* Mitchell and Wallace, 1992). The problem is particularly complicated for the Gulf of Guinea. This oceanic region straddling the equator is limited by the African continent to the north and entirely open toward the south. As a result of this meridional asymmetry, the Gulf of Guinea is mainly under the climatic influence of the austral hemisphere.

Though local wind forcing (primarily meridional) can theoretically contribute to oceanic dynamics in the Gulf of Guinea (Cane and Sarachik, 1977; Philander and Pacanowski, 1981), it does not seem strong enough to be the sole cause of the large observed oceanic variability (Houghton, 1976; Bakun, 1978). On a seasonal time scale, results from a reduced-gravity ocean model (Busalacchi and Picaut, 1983) indicate that the observed zonal wind stress in the western equatorial Atlantic can account for much of the observed variability in the thermal structure of the Gulf of Guinea. Furthermore, a statistical study of observed deviations from the seasonal cycle (Servain *et al.*, 1982) indicates that surface wind anomalies in the western equatorial Atlantic precede by a few weeks SST anomalies in the Gulf of Guinea. In agreement with the remote forcing hypothesis, Katz (1987) observed pulses of thermocline displacement propagating eastward along the equator. Recently, similar displacements during the northern spring-time were noted from sea level measurements by the GEOSAT altimeter (Arnault and Cheney, 1994).

The ocean dynamics of this remote forcing are mostly related to a blended pattern of baroclinic waves forced by changes in the wind stress (Moore and Philander, 1977; Moore *et al.*, 1978). Sudden changes in the zonal wind stress along the equator off the coast of Brazil are highly effective in forcing thermocline displacements along the equator. Packets of Kelvin waves propagate eastward along the equatorial guide, crossing the basin in somewhat over a month. They then rebound from the African coast in a mixed system of poleward coastal Kelvin waves and slow westward Rossby waves (McCreary *et al.*, 1983). Such propagating baroclinic processes induce abnormal variations in the subsurface thermal structure, directly detectable with some delay (a few days to a few weeks) because the thermocline shallows or deepens in opposite phase to the sea level.

An extremely shallow thermocline means a reinforced upwelling, expressed by additional shrinking of subsurface oceanic layers. Conversely, a deepening thermocline means an increase of subsurface heat storage associated with thermal expansion of these layers. Thus, these dynamical processes (shrinking or deepening of the subsurface layers) can be followed by additional cooling or warming of the surface. In fact the SST variability is not directly related to the dynamic height variability, but is also driven by the local air-sea heat exchange, advection... Nevertheless, because this heat budget variability is function of the winds, the correlation between the SST anomaly and the dynamic height anomaly is generally high, particularly in the tropics (Rao *et al.*, 1989, Mc Creary *et al.*, 1993). Thus, especially in the Gulf of Guinea during the upwelling season (July to September), an abnormal lowering (rise) of sea level (or dynamic height) follows a strengthening (relaxation) of wind stress in the western region, and is related to later negative (positive) SST anomalies. In the following sections we provide an illustration of this relationship, with the particularly large warm episode which occurred in the equatorial Atlantic during 1968.

DATA AND MODEL

Wind stress and SST data were deduced from January 1964 to May 1994 observations routinely obtained in the tropical Atlantic Ocean by selected ships. The processing used to obtain pseudo-stress and SST monthly fields on a regular grid (2° longitude x 2° latitude) with no gaps is described in Picaut *et al.* (1985, hereafter noted PS; see also subsequent presentations in Servain *et al.*, 1987, and Servain and Lukas, 1990). Briefly, this method is based on a combination of objective and subjective analysis. The data are first averaged in 2° latitude by 5° longitude boxes. Statistical tests are then applied on individual values within each

box. They are based on comparisons with climatology and values of surrounding boxes, according to which some data are rejected or corrected. This procedure does not result in rejecting dramatic abnormal events. An objective analysis method of the successive-correction type (Cressman, 1959) is then used to create the 2° x 2° gridded monthly fields.

The ocean numerical model used here computes the linear response of the tropical Atlantic Ocean to the wind forcing on three baroclinic vertical modes. Indeed, du Penhoat and Treguier (1985) have shown from a model with 9 modes that 95 % of the signal is contained in the first three modes. Furthermore, du Penhoat and Gouriou (1987) demonstrated that this category of model reproduces interannual dynamic height topography variability at a much lower cost than 3D-primitive equation models. The model run captured the 1983-84 variability in the tropical Atlantic Ocean quite well, with the abnormal warm event in 1984 characterized by a huge change in the zonal equatorial sea level slope compared to 1983. The decomposition in vertical modes is obtained from a mean density profile, characteristic of the mid-equatorial Atlantic Ocean (24°W). The phase speeds associated with the first 3 modes are respectively 2.18, 1.32 and 0.89 ms^{-1}. These linearized equations are discretized on a staggered grid (Arakawa type C) defined by trigonometric functions resulting in a variable grid spacing, with higher resolution where it is important for the wave dynamics. The basin extends from 20°N to 20°S in latitude and from 60°W to 13°E in longitude. In longitude, the smallest mesh size (50 km) is near the African and American coasts, increasing to 115 km in the center of the basin. In latitude, the smallest mesh size is at the equator (50 km) to correctly resolve the equatorial radius of deformation. At the northern and southern boundaries, the mesh size is 85 km. No slip boundary conditions have been used on coastal, northern, western and southern

frontiers. The horizontal diffusivity coefficient is 10^3 m^2s^{-1}. A variable time-step (one, two and four hours respectively for the first, second, and third modes) is incorporated for the time integration of the model. The model has been spun up over 17 years by the climatological Hellerman and Rosenstein's (1983) wind stress, at which point, the model had a regular seasonal cycle of the 0/500 dbar dynamic height computed from the pressure field.

A control run of the linear model was first performed from January 1964 to May 1994 using the observed monthly wind stress fields prepared by PS and subsequent works. The wind forcing is linearly interpolated at the variable time-step of the model, and so that the time-step of the model outputs can be chosen indifferently between 4 hours and one month. We chose in this study to use bi-monthly averages obtained from the original model outputs.

THE WIND STRESS-DYNAMIC HEIGHT-SST LAGGED RELATIONSHIP IN THE TROPICAL ATLANTIC

In Figure 1, we present fields of the 3-month average centered over May 1968 of the observed wind stress anomaly (Fig. 1a), of the 3-month average centered over June 1968 of the linearly simulated dynamic height anomaly pattern (Fig. 1b), and of the 3-month average centered over July 1968 of the observed SST anomaly (Fig. 1c). The 1968 anomalous event emerged around May, with a considerable relaxation (20 m^2s^{-2}, *i.e.*, about 50 10^{-3} Pa) of the wind stress in the western equatorial region. The linear model simulation, forced by this observed wind, subsequently (around June) presents an anomalous elevation (+ 5 cm.dyn) of the simulated dynamic height centered in the Gulf of Guinea, and a decrease (-10 cm.dyn) of dynamic height in the western region. This particular dynamic

height pattern was followed a few weeks later (around July) by an equatorially-trapped SST warming (up to 1.5 °C) in the Gulf of Guinea.

The 1968 warm event was not unique within the last decades. In an attempt to find statistically whether they follow a common pattern, a series of zero-lag and lagged correlation analyses were completed for the 1964-1993 observed SST and wind stress, and for the simulated dynamic height derived from the control run of the linear model. Our purpose is to deduce suitable relationships for the Gulf of Guinea, first between northern summer SST and the immediately preceding dynamic height, and then between this dynamic height and immediately preceding wind stress. The computations are made between one time series at a specific point in the Gulf of Guinea and one of the other (or the same) variable at all points of the tropical basin. The particular site was arbitrary chosen at 4°W along the equator (directly south of Abidjan). Such a choice resulted from the combination of two arguments: (*i*) 4°W/Equator is very close to the nodal point of the equatorial upwelling (*e.g.* see PS, p. 78) which is generally located at 9°W/Equator (the correlation coefficients between both locations for anomalies of SST and dynamic heights are up to 0.97); (*ii*) 4°W/Equator was often the site of hydrographic measurements and moorings (*e.g.*, Houghton and Colin, 1986). The correlation computations are summarized by mapping 2D correlation coefficients, which are scalar values (SST with itself or SST with dynamic height), or are complex values (dynamic height with the x-y components of wind stress). All computations were done from the set of 30 individual years, using the 3-month average anomaly of each variable centered around a specific month. Coefficients of up to |0.3| (simple correlation) or |0.4| (complex correlation) are roughly significantly non-zero up to the 95 % confidence level. Only the zero-line and

isolines related to these and higher coefficient values are plotted in the following figures for a selection of the results.

Figure 2 represents a zero-lag correlation pattern performed between the SST anomaly at the point 4°W/Equator and SST anomalies in the tropical basin for the 3-month average centered over July, when the SST anomalies are the largest. The large area of high positive coefficient (up to + 0.5) indicates that the point 4°W/Equator is representative of northern summer SST variability in the entire Gulf of Guinea. The same conclusion is reached for the simulated dynamic height centered over June (not illustrated here, but the structure in Fig. 1b is representative of typical deviations).

Figure 3a shows the lagged relationship between the observed SST anomaly around July throughout the basin and the simulated dynamic height anomaly around June at 4°W/Equator. For comparison, we also present the zero-lag correlation pattern (Fig. 3b) with both SST and dynamic height anomalies taken around July. As expected, the SST anomaly throughout the Gulf of Guinea is positively correlated with the dynamic height anomaly at 4°W/Equator, though the noted coefficients are not very large (about + 0.3-0.5): a warmer (colder) temperature being associated with a rise (lowering) of the sea surface level in the same region. A relative weakness in the positive values of the correlation coefficient illustrates the fact that these two variables are not directly connected. Nonetheless, the highest correlation coefficients can be noted in Figure 3a (up to + 0.5), demonstrating that such a relation is clearly most relevant when an abnormal dynamic height precedes an abnormal SST pattern by a few weeks.

The complex lagged correlation pattern between the simulated dynamic height anomaly centered over June, at 4°W/Equator, and the wind stress anomaly around May throughout the tropical basin is presented in figure 4a. We also

present (Fig. 4b) the zero-lag correlation pattern when both dynamic height and wind stress anomalies were taken around June. We represent the bidimensional correlation by vectors whose length is proportional to the norm of the complex coefficients. The isolines of the vector norms, here multiplied by 100, are superimposed on the vector fields. To interpret those fields, it is interesting to compare them with the vectorial wind stress around climatic averages May and June (*e.g.*, see Servain and Lukas, 1990, pages 6 and 7): northeast and southeast trade winds converge in an intertropical convergence zone (ITCZ) schematised by a thick discontinuous line in Figures 4a,b. In the western part of the basin the ITCZ slowly migrates meridionally from a purely equatorial position in May to approximatly 4°N in June. Throughout the year in the eastern Gulf of Guinea, the southeast trade winds progressively veers to the right when crossing the equator, reaching the African coast in a southwesterly direction. These features are characteristic of the African monsoon which is most intense during boreal summer.

A main feature evident in both Figures 4a and 4b is located west of 10°W and relates to a northwesterly disturbance along and immediately south of the ITCZ. This explains why a dramatic anomalous relaxation (intensification) of the wind system in that region, as seen in the example of figure 1a, is strongly correlated (complex coefficients up to 0.9) with an anomalous rise (decrease) of the dynamic height at 4°W/Equator. A second important common feature corresponds to a northerly perturbation along the African coast, indicating that a substantial reduction (increase) in the monsoon is also significantly correlated (complex coefficients up to 0.5) with an anomalous rise (decrease) of dynamic height immediately to the south. Another characteristic of both Figures 4a and 4b, which has less statistical significance than the first two features, is that the

disturbance pattern has the same cyclonicity in the north and south studied basins, with the strongest signature located in the north-east and south-east respectively. The large weakening of the wind stress in the vicinity of Cabo Verde Islands (20°W/20°N), where the wind convergence is maximum at this time of the year (*e.g.* see Hastenrath and Lamb, 1977, charts 34-35), further relates to an abnormal cyclonicity.

Here again the lagged correlation coefficients are generally greater than those related to the zero-lag relation, suggesting that one can generalize for the last 30-year period the previously noted coupled behaviour between wind stress, dynamic height and SST anomalies in the tropical Atlantic during the northern spring-summer season. As oceanographers, we were therefore particularly interested in investigating the predictability of anomalous climatic events in the Gulf of Guinea. We will present that in the following section.

Hereafter we retain the grid point at 4°W/Equator to illustrate the variability in the Gulf of Guinea.

FORECASTING THE VARIABILITY OF DYNAMIC HEIGHT

The bi-monthly time series of the simulated dynamic height anomaly at 4°W-Equator is presented in Figure 5. The anomalies are the departure of the bi-monthly outputs of the control run from the bi-monthly climatological averages computed for the 1964-1993 period. As was earlier discussed, most of the largest simulated dynamic height anomalies at 4°W-Equator should be associated in the Gulf of Guinea either with an observed warm event (examples 1968 and 1984) or with an observed cold event (examples 1982-83 and 1992).

Forecasts were performed for each individual year during the 1964-1994 period using the observed wind forcing from January to May, then retaining the

May wind stress for three months. This provides a forecast of dynamic height anomaly during the three months June-to-August, which is compared (except for 1994) with that from the control run for the same period. In Figure 6 we show the June-to-August averages of dynamic height anomalies at 4°W-Equator, deduced from the 1964-1993 control run (filled circles) and from the 1964-1994 test runs (open circles). The correlation coefficient for the 30 individual years between control and forecasts is 0.55. We added on this figure the 3-month averages centered over July of observed SST anomalies at 4°W/Equator (asterisks). Different features emerge from Figure 6. First, it is encouraging that for practically all the yearly cases the sign of the forecast anomalies is the same as that of the control run. Furthermore, the largest simulated deviations in the control run are correctly predicted by the test runs. This is true for large positive occurrences as in 1964, 1966, 1968, 1984 and 1989, as well as for large negative occurrences, as in 1976, 1982, 1983, 1986 and 1988. Poor forecasts occur mainly when deviations in the control run are small, as for instance in 1972, 1974, 1978, 1979, 1991 and 1992. For only two cases (1969 and 1987), the forecast is bad whereas simulated values provided by the control run are relatively large.

As was earlier discussed in the paper, the zero-lag correlations between the observed SST anomalies (asterisks) and the dynamic heights anomalies simulated by the control run (filled circles) and test runs (open circles) are positive but relatively weak (0.30 and 0.28 respectively). Although we found in the preceding section that this correlation is a little bit higher (about 0.45) at a one-month lag (see on Fig. 3a), this would not be sufficient to produce a good forecast skill for SST anomalies using a scheme combining the linear oceanic model and statistical computations. Instead of this approach, we will make qualitative comments on SST anomalies during the boreal summer in the Gulf of Guinea. We note for

about two thirds of the cases (20 years out of 30 years) that the sign of the observed SST anomalies at 4W/Equator during the boreal summer corresponds to the sign of the simulated dynamic heights (both for control run and forecast). However, this does not hold during the three years 1986-87-88. That may be due to problems with the wind data and/or to some particularly strong interannual signal in the heat budget.

One intriguing feature in Figure 6 is that predicted dynamic height anomalies at 4°W/Equator are often much larger than dynamic height anomalies deduced from the control run. This is especially salient for some years, such as 1968 and 1974. We will try to explain this by the following argument based on remote forcing. Because May wind stress is repeated three times, the predicted July-to-August dynamic height anomalies are all larger when May wind stress anomaly forcing is itself the largest. This persistence effect is reinforced when the stress anomaly is already stronger in the same way during the early months. In Tables 1 and 2, we report the bi-monthly averages of dynamic height anomalies at 4°W/Equator: the total year values for the control run (Table 1), and the January-to-August values for test runs (Table 2). Note that the curves in Figure 6 are derived from a time integration of the June-to-August shaded columns of Tables 1 and 2. Based on remote forcing ideas, a line-by-line reading of Tables 1 and 2 provides for each year an explanation for the difference between dynamic height anomalies in the control run and forecast, as seen in Figure 6. Here, we shall restrict the discussion to two outstanding situations: the rightly predicted 1968 event (with high dynamic height anomalies for both the control run and the 1968 test run) and the improperly predicted 1974 event (with a very high dynamic height anomaly from the 1974 test run versus a close-to-zero dynamic height anomaly from the control run). In 1968, the control run (Table 1) exhibits strong

positive dynamic height anomalies throughout the period from February until August, resulting from a persistent abnormal weakness of the zonal wind stress during the entire first half of this year (see PS, pages 178 to 192). This is obviously quite appropriate to obtain an accurate forecast, as indicated in Figure 6 and Table 2. In 1974 on the contrary, the control run (Table 1) displays weak dynamic height anomalies during the period from February to April, then strong positive dynamic height anomalies in May-June, and again weak dynamic height anomalies in July-August. This pattern is associated with variable conditions in wind stress anomaly during the first half of 1974 when an important westerly perturbation occurred *only* during April-May (see PS, pages 322 to 338). Obviously, retaining this large value for the three subsequent months leads to a very high anomaly of dynamic height, therefore a poor forecast (Fig. 6 and Table 2). A full set of other circumstances, intermediate between the well-predicted 1968 event and the poorly predicted 1974 event, can be found in Tables 1 and 2.

1983 and 1984 are well-known opposite examples of SST anomalies in the Gulf of Guinea during the boreal summer (Philander, 1986). From Servain *et al.* (1987), negative SST anomalies of about -1.5°C extended in the eastern equatorial domain from May to July 1983, whereas during the following year, positive SST anomalies with a magnitude larger than +2.5°C remained in the far eastern Gulf of Guinea during at least five months starting in June. Figures 7 and 8 show the two simulated dynamic height anomaly patterns in the entire tropical basin for the years 1983 and 1984. Again this was previously largely documented (du Penhoat and Gouriou, 1987; Verstraete and Vassie, 1990; Reverdin *et al.*, 1991; Delecluse *et al.*, 1994). Figures 7a and 8a are constructed from the control run, while figures 7b and 8b are constructed from the forecast. In each case we performed a time-averaging over the three months June-to-August. The abnormal decrease

(increase) of the simulated dynamic height in the Gulf of Guinea during the northern summer of 1983 (1984) is correctly predicted. The 5-7 dyn.cm elevation of the sea surface in the Gulf of Guinea in the summer of 1984 in comparaison to the summer of 1983 is in the same range as the one observed during the FOCAL/SEQUAL programme (du Penhoat and Gouriou, 1987; Reverdin *et al.*, 1991). This feature is associated with a deepening (10-15 dyn.cm) of the simulated dynamic height in the western equatorial basin in 1984 versus 1983, showing a good relationship with the observed change in the equatorial slope of the sea surface during these two years.

Figures 9 and 10 are respectively related to the standard deviation (SD) and root mean square (RMS) variability of the 1964-1993 simulated dynamic height anomaly. SD is deduced from the control run alone, while RMS is computed from the test runs minus the control run. The unit is in dyn.cm for both SD and RMS. The deduced skill factor (dimensionless) is the ratio of RMS to SD (Fig. 11). In fact, the skill factor can be seen as a seasonal normalisation of RMS. It indicates whether the predicted mode is relevant (skill < 1) or inappropriate (skill > 1) against the control run. All these factors are computed for 1964-1993 and mapped according to each of the six individual fortnights, constituting the three months June-to-August. SD values are nearly constant throughout the study period (Fig. 9). For example in the Gulf of Guinea, SD averages are about 2 dyn.cm, with only a slight increase after mid-July. The lowest RMS values (Fig. 10) are found during the first fortnight of June (RMS < 1 dyn.cm). Then, RMS increases progressively, reaching 2-3 dyn.cm in August for the eastern part of the Gulf of Guinea. The skill maps (Fig. 11) display both positive and negative results. The forecasting mode is fully promising until mid-July, the skill values being less than 1 in almost the entire basin. Beyond mid-July, the forecast mode seems to fail

along the eastern equatorial band with the skill factor there exceeding one. However, the skill factor remains less than 1 during the six fortnights in a few limited areas, such as those in the eastern basin which are symmetrical with respect to the equator at about 12 degrees of latitude. The relatively fast diminution (less than six weeks) of the skill along the eastern equator, as well as the residual low values of this factor for the two poleward eastern regions, is accounted for by wave dynamics discussed earlier. Because equatorially trapped Kelvin waves, generated by a wind perturbation in the western part of the basin, propagate eastward, reaching the African coast in about a month (Moore *et al.*, 1978; Carton and Huang, 1994), we expect that the forecast would not.be relevant beyond four or six weeks along the equator in the Gulf of Guinea. The response in the subtropical eastern regions is more related to a steady process involving Ekman pumping and slow westward Rossby waves (Mc Creary *et al.*, 1983; Carton and Huang, 1994), so that the forecast can be exploited there for a longer time.

SUMMARY AND CONCLUDING REMARKS

This work was undertaken as a pilot study to forecast abnormal climatic events over the tropical Atlantic. The framework of the numerical experiment was adopted assuming some commonly accepted hypotheses based on prior empirical analyses of sea surface variables in the equatorial Atlantic. These earlier studies indicated that it would be possible to predict warm or cold events in the Gulf of Guinea during the northern summer, provided the wind during the northern spring be known. Our first aim was to quantify these lagged relationships over a long time period. Three variables were statistically analysed during the years 1964-93(94) for the tropical Atlantic: two variables from surface observations (monthly

wind stress and SST) and the third (dynamic height) from a linear oceanic model (control run), itself forced by the observed wind stress. This analysis confirms that (*i*) a large-scale wind-stress anomaly around May correlates well with the June dynamic height anomaly in the Gulf of Guinea and (*ii*) a June dynamic height anomaly in the Gulf of Guinea correlates well with the local SST anomaly in July. Furthermore, it is shown that these lagged relationships are more significant than zero-lag relationships. Wind perturbation during northern spring, which induces an oceanic response in the Gulf of Guinea during the following months, originates mainly from three complementary effects. The first, with the highest dynamical consequence, is located in the western equatorial basin and is the main remote forcing of the eastern Atlantic dynamic height. The second is located along the northern coast of the Gulf of Guinea, and corresponds to the monsoon effect which is basically related to meridional fluctuations in air flow circulations. The third is associated with an abnormal cyclonicity in both the southern and northern basins, with an action center in the vicinity of Cabo Verde Islands.

Based on the results of these empirical analyses, we performed a numerical forecasting experiment specifically to simulate the dynamic height in the Gulf of Guinea. The linear oceanic model was again used, but this time the forcing was assumed to persist during three additional months from May of each of the years 1964-1994. The resulting dynamic height anomalies related to these three months were considered as a forecast for the months June to August and compared (except for 1994) to the dynamic height anomalies provided by the control run.

We conclude that, as of early June of each year of the last three decades, it would have been possible to predict the correct sign of the dynamic height anomaly in the Gulf of Guinea during the northern summer. Besides, the largest dynamic height anomalies in the control run during the last 30 years have been

correctly forecast, though sometimes a little more intense than in the test run. This supports the idea that the prediction of highly abnormal summer dynamic height in the Gulf of Guinea can be based on wind information during the previous spring. It was also concluded that the most appropriate areas for forecasting the summer dynamic height anomalies are located in the eastern basin on both sides of the equator at approximately 12 degrees of latitude, *i.e.* in oceanic regions where the dynamics are moving slower compared to those related to the equatorial wave guide.

Because of the high positive relationship between anomalies of dynamic height and SST, once the dynamic height anomaly is forecasted, one could predict the sign of the SST anomaly in the same region. Based on the observed SST anomalies in the Gulf of Guinea during the last 30 boreal summers, we actually noted that this prognosis was valid for 20 summers.

However, some model deficiencies were noted, which can be explained by the linear theory on which the present forecasting simulation is based. Thus, some large dynamic height anomalies should have been predicted whereas the anomalies provided by the control run remained small and insignificant. This occurred when a strengthening wind perturbation in May vanished or even reversed during the following months. In this instance, the wind persistent assumption of the forecasting experiment is not producing a suitable summer oceanic response. Furthermore, it has been statistically noted that accurate forecasts along the equator do not last for more than about six weeks, which obviously limits the usefulness of the forecast. Fortunately, the largest anomalous events usually are multi-month processes (*e.g.* 1968, 1976 or 1984), which can be forecasted for a longer time.

The accuracy of the forecasting method was compared with the skill of persistence of the dynamic height anomaly in the control run. Six series of test runs were implemented to forecast six calendar months equally spread out all along the year (from February to December). Only the results related to the point 4W/Equator are shown here with two sets of correlation coefficients (Fig. 12). A first set (stars) deduced from the control run gives the correlation between simulated dynamic height anomalies in two successive months, which supplies the one-month persistence information. The second set (circles) is the correlation between test runs and control run for the exact calendar month, which supplies the accuracy of the forecasting method. The computations are completed for each of the six calendar months, symbolized along the x-axis by FEB, APR, and so on. In any case, the simulated one-month forecast is better than the deduced one-month dynamic height persistence. Further informations can also be gathered from figure 12: (*i*) a seasonal evolution is noted in the accuracy of the two methods, though with a better steadiness for the forecast method; (*ii*) for both methods, the best performance occurs for a prediction of June, and the worst for a prediction of October (though with a very small difference between the two extreme values in the case of the forecasting method). This series of results suggests that the proposed forecasting method can be used in the Gulf of Guinea for all seasons, albeit with a better chance of succeeding during the onset of the seasonal equatorial upwelling.

The modelling forecast presented here could be considerably improved. For example, combining the linear oceanic model presented here with a simple statistical method using the lagged statistical relation established between dynamic height and SST anomalies, could be used to forecast SST anomalies. Further advanced statistical methods, such as those using canonical correlation

analyses (*e.g.* Barnett and Preisendorfer, 1987) or PIPs approach (Hasselman, 1988) could be also attempted. Another alternative, which has our preference, involves the choice of an Ocean Global Circulation Model (OGCM). In such a 3-D model as that one developed by LODYC (Chartier, 1985), SST *is* a simulated variable. However, early versions of the LODYC model code were not sufficiently accurate for assessment of the interannual SST signal (Servain *et al.*, 1994), which is one reason why in this pilot study we opted for a simpler and much cheaper model. The latest versions of the LODYC model (Blanke and Delecluse, 1993) highlight the complex behaviour of turbulent mixing in the ocean, which leads to a significant improvement in the simulated SST, especially along the equator. This new version of the model code will soon be used in forecasting experiments for similar situations to those described in the present study. Last but not least, we expect in the near future to use a coupled ocean-atmosphere model (CGCM). At this time, coupled models have only been tested over the Pacific ocean.

All the results of this study lead us to confirm an idea already stated in earlier works: the northern spring-summer period is particularly crucial for observing and forecasting abnormal events in the Gulf of Guinea. Thus, we recommend that a particular attention should be devoted to observations (wind, sea level, SST, etc.) during the decisive period from March to August in the equatorial Atlantic. This survey could be made with a *dedicated* monitoring analysis relying on *in-situ* observations provided by ships of opportunity in operational mode over the Global Telecommunication System (GTS), and on remote observations of wind stress and sea level provided by present and future satellites (ERS1, ERS2, TOPEX-POSEIDON, etc.).

Acknowledgments: We are very grateful to Tony Busalacchi and Gilles Reverdin for their help in finalizing our draft.

References

Arnault, S., and R.E. Cheney. Tropical Atlantic sea level variability from GEOSAT (1985-1989), *J. Geophys. Res.*, **99**, 18,207-18,223, 1984.

Bakun, A., Guinea current upwelling, *Nature*, **271**, 147-150, 1978.

Barnett, T.P. and R. Preisendorfer. Origins and levels of monthly and seasonal forecast skill for United States surfaces air temperatures determined by canonical correlation analysis, *Mon. Weath. Rev.*, **115**, 1825-1850, 1987.

Barnett, T.P., N. Graham, M. Cane, S. Zebiak, S. Dolan, J. O'Brien, and D. Legler. On the prediction of the El Niño of 1986-87, *Science*, **241**, 192-196, 1988.

Blanke, B., and P. Delecluse. Variability of the tropical Atlantic Ocean simulated by a general circulation model with two different mixed-layer physics, *J. Phys. Oceanogr.*, **23**, 1363-1388, 1993.

Busalacchi, A.J., and J. Picaut. Seasonal variability from a model of the tropical Atlantic Ocean, *J. Phys. Oceanogr.*, **13**, 1564-1588, 1983.

Cane, M.A., and E.S. Sarachik. Forced baroclinic ocean motions. II. The linear equatorial bounded case, *J. Mar. Res.*, **35**, 395-432, 1977.

Cane, M.A., and S.E. Zebiak. A theory for El Nino and the Southern Oscillation, *Science*, **228**, 1085-1087, 1985.

Carton, J.A., and B. Huang. Warm events in the tropical Atlantic. *J. Phys. Oceanogr.*, **24**, 888-903, 1994.

Chartier, M., *Un modèle numérique tridimensionnel aux équations primitives de circulation générale de l'océan*, Thèse de doctorat d'Université, Univ. P. et M. Curie, Paris, France, 111 pp., 1985.

Cressman, G.P., An operational objective analysis system, *Mon. Weath. Rev.*, **87**, 367-374, 1959.

Delecluse, P., J. Servain, C. Levy, L. Bengtsson, and K. Arpe. On the connection between the 1984 Atlantic warm event and the 1982-1983 ENSO, *Tellus*, **46A**, 448-464, 1994.

du Penhoat, Y., and A.M. Treguier. The seasonal linear response of the tropical Atlantic ocean, *J. Phys. Oceanogr.*, 15, 316-329, 1985.

du Penhoat, Y., and Y. Gouriou. Hindcasts of equatorial sea surface dynamic height in the Atlantic in 1982-1984, *J. Geophys. Res.*, **92**, 3729-3740, 1987.

Fonteneau, A., Les anomalies de l'environnement en 1984 dans le Golfe de Guinée. Effets possibles sur la capturabilité de l'albacore, *Rec. Doc. Scient. ICCAT*, **36**, 380-408, 1991.

Hasselman, K, PIPs and POPs: The reduction of complex dynamical systems using principal interaction and oscillation patterns, *J. Geophys. Res.*, **93**, 11,015-11,021, 1988.

Hastenrath, S., and L. Heller. Dynamics of climate hazards in northeast Brazil, *Q. J. R. Meteorol. Soc.*, **103**, 77-92, 1977.

Hellerman, S., and M. Rosenstein. Normal monthly wind stress over the world ocean with error estimates, *J. Phys. Oceanogr.*, **13**, 1093-1104, 1983.

Hisard, P., El Niño response in the tropical Atlantic Ocean during the 1984 year. in *International Symposium of Long Term Changes Mar. Fish Pop. 1986*, T. Wyatt and M.G. Larraneta; editors. Vigo,273-290, 1988.

Houghton, R.W., Circulation and hydrographic structure over the Ghana continental shelf during the 1976 upwelling, *J. Phys. Oceanogr.*, **6**, 909-924, 1976.

Houghton, R.W., and C. Colin. Thermal structure along 4°W in the Gulf of Guinea during 1983-1984, *J. Geophys. Res.*, **91**, 11727-11739, 1986.

Inoue, M., and J.J. O'Brien. A forecasting model for the onset of a major El Niño, *Mon. Weather Rev.*, **112**, 2326-2337, 1984.

Katz, E.J., Equatorial Kelvin waves in the Atlantic, *J. Geophys. Res.*, **92**, 1894-1898, 1987.

Latif, M., and M. Flügel. An investigation of short range climate predictability in the tropical Pacific, *J. Geophys. Res.*, **96**, 2661-2673, 1991.

Leetmaa, A., and M. Ji. Operational hindcasting of the tropical Pacific, *Dyn. Atmos. Oceans.*, **13**, 465-490, 1988.

McCreary, J.P., J. Picaut and D.W. Moore. Effect of annual remote forcing in the eastern tropical Atlantic, *J. Mar. Res.*, **42**, 45-81, 1983.

McCreary, J.P., P.K. Kundu, and R.L. Molinari. A numerical investigation of dynamics, thermodynamics and mixed-layer processs in the Indian Ocean, *Prog. Oceanog.*, **31**, 181-244, 1993.

Merle, J., Seasonal heat budget in the equatorial Atlantic Ocean, *J. Phys. Oceanogr.*, **10**, 464-469, 1980.

Merle, J., M. Fieux, and P. Hisard. Annual signal and interannual anomalies of sea surface temperature in the eastern equatorial Atlantic, Gate Sup. II, *Deep-Sea res.*, **26**, 77-101, 1980.

Mitchell, T.P., and J.M. Wallace. The annual cycle in equatorial convection and sea surface temperature, *J. Climate*, **5**, 1140-1156, 1992.

Moore, D.W., and S.G.H. Philander. Modeling of the tropical oceanic circulation, *The Sea*, **6**, E.D. Goldberg, I.N. McCave, J.J. O'Brien, and J.H. Steele, Eds., Wiley Interscience, 319-361, 1977.

Moore, D.W., P. Hisard, J. McCreary, J. Merle, J. O'Brien, J. Picaut, J.M. Verstraete, and C. Wunsh. Equatorial adjustment in the eastern Atlantic, *Geophys. Res. Lett.*, **5**, 637-640, 1978.

Moura, A.D., and J. Shukla. On the dynamics of droughts in northeast Brazil: Observations, theory and numerical experiments with a general circulation model, *J. Atmos. Sci.*, **38**, 2653-2675, 1981.

Philander, S.G.H., Variability of the tropical oceans, *Dyn. Atm. Ocean*, **3**, 191-208, 1979.

Philander, S.G.H., Unusual conditions in the tropical Atlantic ocean in 1984, *Nature*, **322**, 236-238, 1986.

Philander, S.G.H., and R.C. Pakanowski. The oceanic response to cross-equatorial winds (with application to coastal upwelling in low latitudes), *Tellus*, **33**, 201-210, 1981.

Picaut, J., J. Servain, P. Lecomte, M. Séva, S. Lukas, and G. Rougier. *Climatic atlas of the tropical Atlantic wind stress and sea surface temperature 1964-1979*, Université de Bretagne Occidentale, Brest, University of Hawaii, Honolulu, 467 pp., 1985.

Reverdin, G., P. Delecluse, C. Levy, P. Andrich, A. Morlière, and J.M. Verstraete. The near surface tropical Atlantic in 1982-1984: Results from a numerical simulation and a data analysis, *Prog. Oceanog.*, **27**, 273-340, 1991.

Rao, R.R., R.L. Molinari, and J.F. Festa. Evolution of the climatological near-surface thermal structure of the tropical Indian Ocean, 1. Description of mean monthly mixed layer depth, and sea surface temperature, surface current, and surface meteorological fields, *J. Geophys. Res.*, **94**, 10,801-10,815, 1989.

Servain, J., Simple climatic indices for the tropical Atlantic Ocean and some applications, *J. Geophys. Res.*, **96**, 15137-15146, 1991.

Servain, J., and S. Lukas. *Climatic atlas of the tropical Atlantic wind stress and sea surface temperature 1985-1989*, Institut Français de Recherche pour l'Exploitation de la Mer, Plouzané, France, 143 pp., 1990.

Servain, J., J. Picaut, and J. Merle. Evidence of remote forcing in the equatorial Atlantic Ocean, *J. Phys.Oceanogr.* , **12**, 457-463, 1982.

Servain, J., J. Picaut, and A.J. Busalacchi. Interannual and seasonal variability of the tropical Atlantic Ocean depicted by sixteen years of sea surface temperature and wind stress, in *Coupled Ocean-Atmosphere Models*, J.C.J. Nihoul Ed., Elsevier, 211-235, 1985.

Servain, J., M. Séva, S. Lukas, and G. Rougier. Climatic atlas of the tropical Atlantic wind stress and sea surface temperature: 1980-1984, *Ocean-Air Interactions*, **1**, 109-182, 1987.

Servain, J, A. Morlière, and C.S. Pereira. Simulated versus observed sea surface temperature in the tropical Atlantic Ocean, *The Global Atmosphere-Ocean System*, **2**, 1-20, 1994.

Verstraete, J.M., and J. Vassie. The equatorial structure of the zonal and meridional pressure gradients in the equatorial Atlantic during 1983 and 1984, *Deep-Sea Res.*, **37**, 1-26, 1990.

Zebiak, S.E., Air-sea interactions in the equatorial Atlantic region, *J. Climate*, **6**, 1567-1586, 1993.

Figure Captions

Figure 1 - (a): Observed wind stress anomaly (m^2s^{-2}; contour interval 10 m^2s^{-2}) averaged during April-May-June 1968. Vectors with amplitude lesser than 5 m^2s^{-2} are not represented. (b): Simulated dynamic height anomaly (dyn.cm; contour interval 1 dyn.cm) averaged during May-June-July 1968. (c): Observed SST anomaly (°C; contour interval 0.5 °C) averaged during June-July-August 1968. Continuous line for positive values, and dashed line for negative values. The location 4°W/Equator is indicated by a small star.

Figure 2 - Point correlation coefficient of the three-month averaged observed SST anomaly centered in July with the simultaneous SST anomaly at 4°W/Equator (continuous line for positive values, and dashed line for negative values). Contour interval is 0.1. Only zero-line and absolute values greater than or equal to 0.3 (95 % of the confidence level) are presented. The location 4°W/Equator is indicated by a small star.

Figure 3 - (a) Point correlation coefficient of the three-month averaged observed SST anomaly centered in July with the three-month average centered on June of the simulated dynamic height anomaly at 4°W/Equator. (b) Point correlation coefficient of the three-month averaged observed SST anomaly centered in July with the three-month average centered on July simulated dynamic height anomaly at 4°W/Equator. Continuous line for positive values, and dashed line for negative values. Contour interval is 0.1. Only zero-line and absolute values greater than or equal to 0.3 (95 % confidence level) are presented. The location 4°W/Equator is indicated by a small star.

Figure 4 - (a) Complex correlation coefficient of the three-month averaged simulated dynamic height anomaly centered in June at 4°W/Equator with the three-month averaged observed wind stress anomaly centered in May. (b) Complex correlation coefficient of the three-month averaged of the simulated dynamic height anomaly at 4°W/Equator centered in June with the in-phase observed wind stress anomaly. Coefficients are multiplied by 100. Contour interval is 10. Only values greater than or equal to 40 (95 % of the confidence level) are represented. Bold dashed lines represent roughly the latitudinal position of the ITCZ during May (a) or June (b) respectively. The location 4°W/Equator is indicated by a small star.

Figure 5 - Bi-monthly time series (January 1964 to May 1994) of the dynamic height anomaly at 4°W/Equator simulated by the control run. The horizontal dotted lines are placed at +/- 1.5 standard deviation (σ).

Figure 6 - Three-month averaged simulated dynamic height anomaly (dyn.cm) centered in July at 4°W/Equator for the control run in 1964-1993 (filled circles), and for the forecast model in 1964-1994 (open circles). Three-month averaged observed SST anomaly (°C) centered in July at 4°W/Equator during 1964-1994 (asterisks).

Figure 7 - Three-month averaged simulated dynamic height anomaly (dyn.cm) centered in July 1983 (contour interval 1 dyn.cm), (a) for the control run, and (b) for the forecast. Continuous line for positive values (*i.e.*, an unusual rise of

dynamic height), and dashed line for negative values (*i.e.*, an unusual lowering of dynamic height).

Figure 8 - As in Fig. 7 but for July 1984.

Figure 9 - (a) to (f): Standard deviation of the dynamic height anomaly (dyn.cm; contour interval 1 dyn.cm) for the 1964-1993 control run for each of the six subsequent fortnights from the beginning of June to the end of August respectively.

Figure 10 - (a) to (f): As in Fig. 9 but for RMS of the difference between dynamic height anomalies in the forecast and the control run in 1964-1993.

Figure 11 - (a) to (f): As in Fig. 9 but for the skill factor (dimensionless): ratio of RMS (Fig. 10) by the standard deviation (Fig. 9). Coefficients are multiplied by 10; contour interval is 2. Dotted line for skill factor below 1.

Figure 12 - Two sets of correlation coefficients between dynamic height anomalies simulated (*i*) by the control run only (stars), and (*ii*) by the control run and the test runs (circles). They represent the one-month persistence effect and the one-month forecast accuracy respectively. Information is only shown for six calendar months: February, April, June, August, October, and December. The vertical bars are related to the 95 % confidence level.

Table Captions

Table 1 - Bi-monthly values from January 1964 to May 1994 for the dynamic height anomaly (dyn.mm) at 4°W/Equator simulated by the control run. Shaded columns correspond to the six fortnights of June-July-August serving as reference to the forecasting model.

Table 2 - Simulated and forecast bi-monthly values for the dynamic height anomaly (dyn.mm) at 4°W/Equator from January to August during the years 1964-1994. Only the shaded colums corresponding to the six fortnights of June-July-August are forecasted.

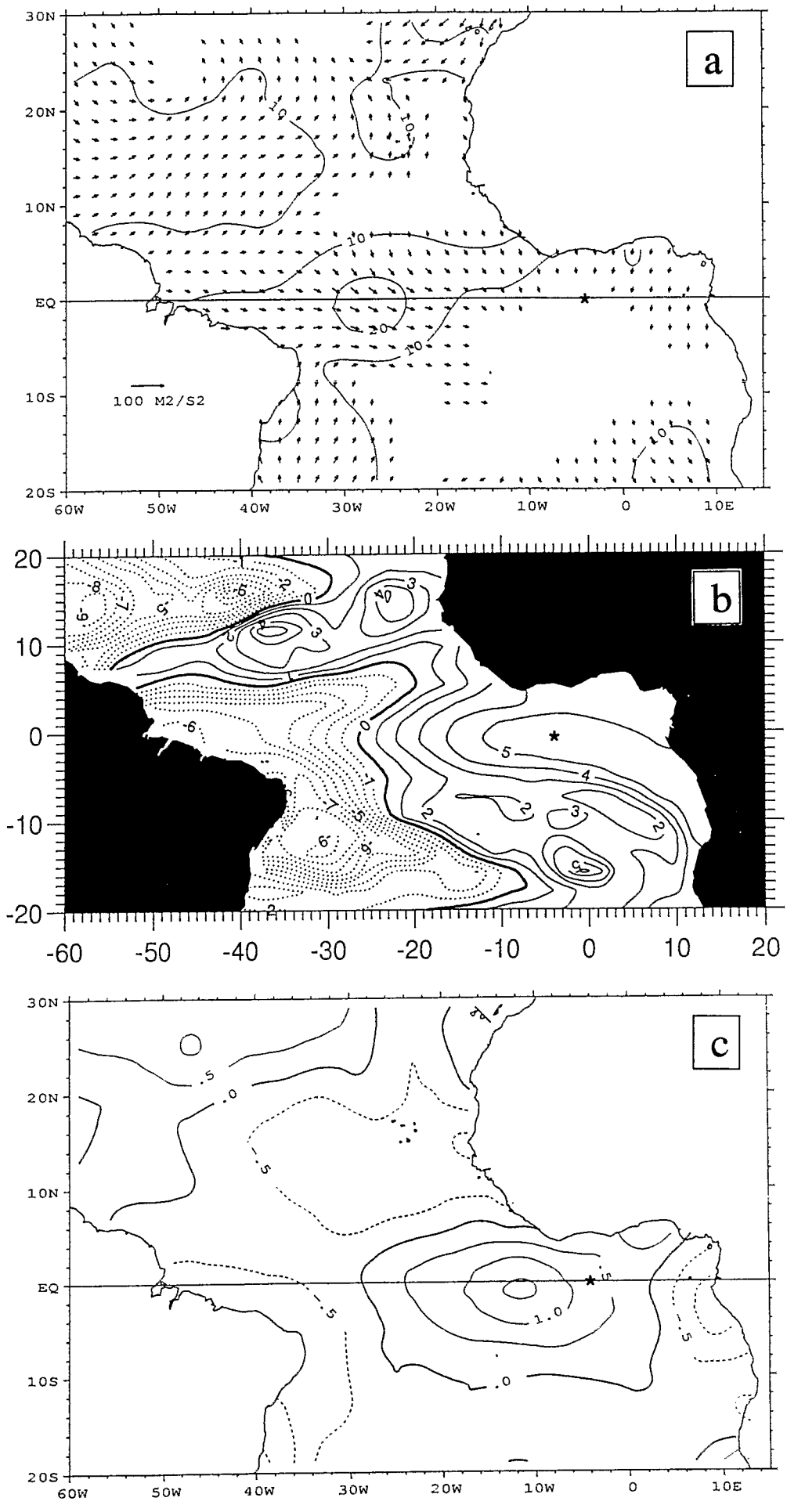
a
30N
20N
10N
EQ
10S
20S
60W
50W
40W
30W
20W
10W
0
10E
100 M2/S2
b
20
10
0
-10
-20
-60
-50
-40
-30
-20
-10
0
10
20
c
30N
20N
10N
EQ
10S
20S
60W
50W
40W
30W
20W
10W
0
10E

Figure 1

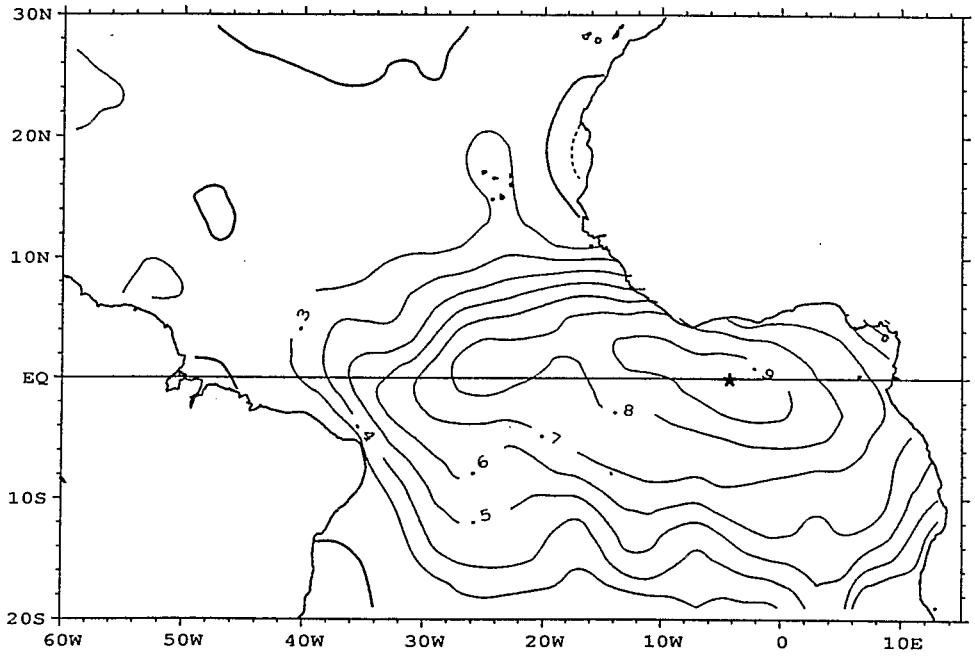

Figure 2

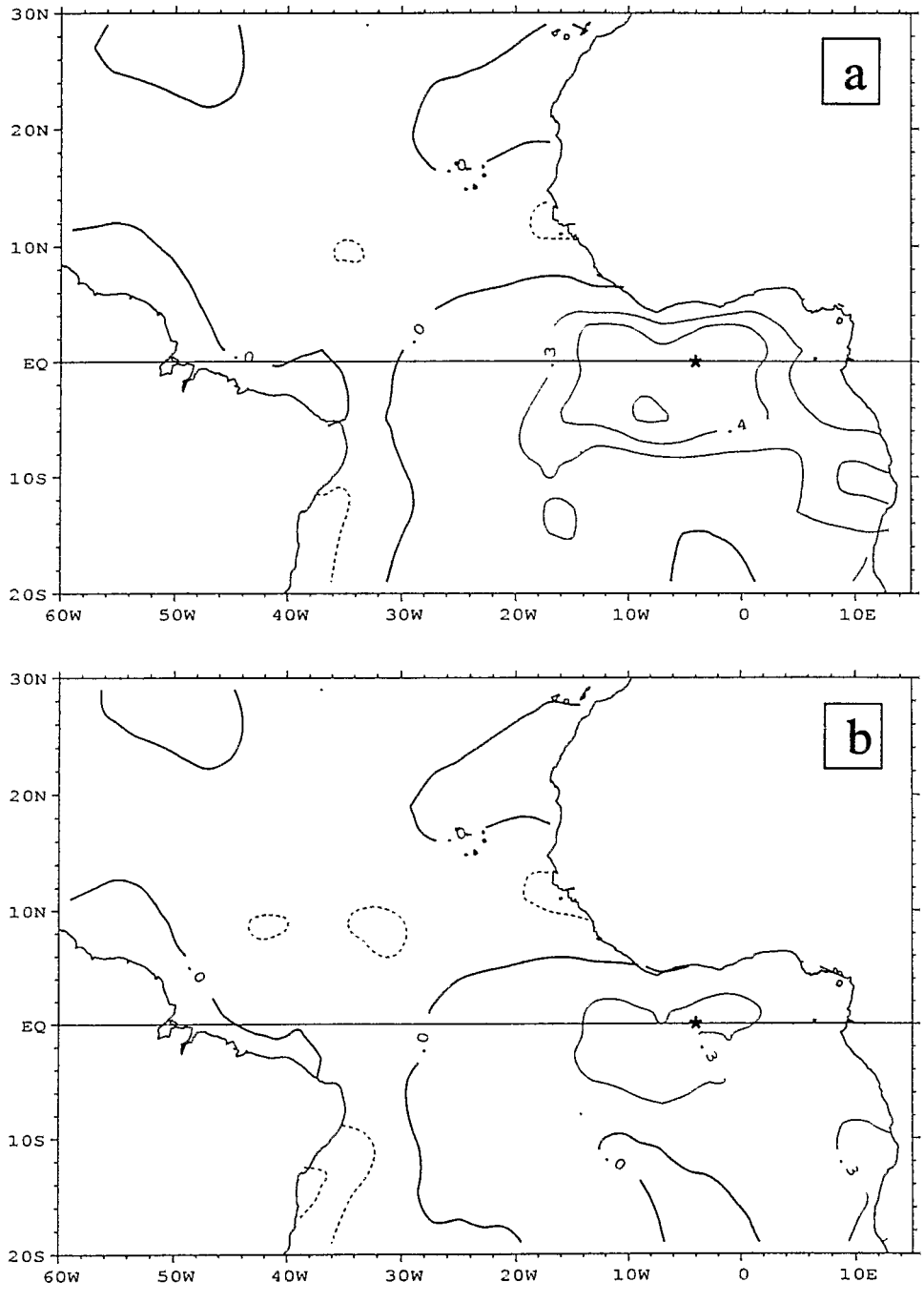

Figure 3

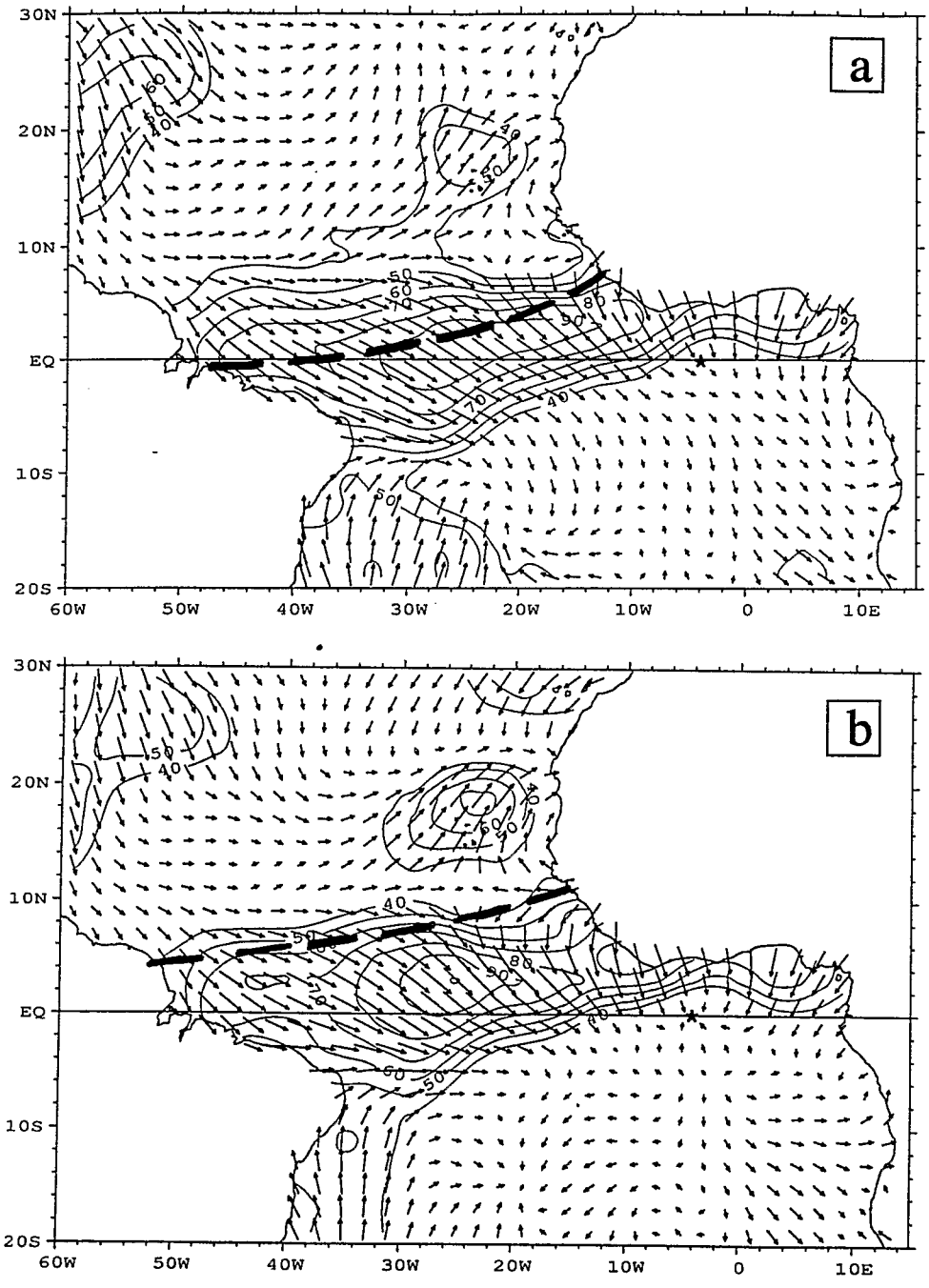

Figure 4

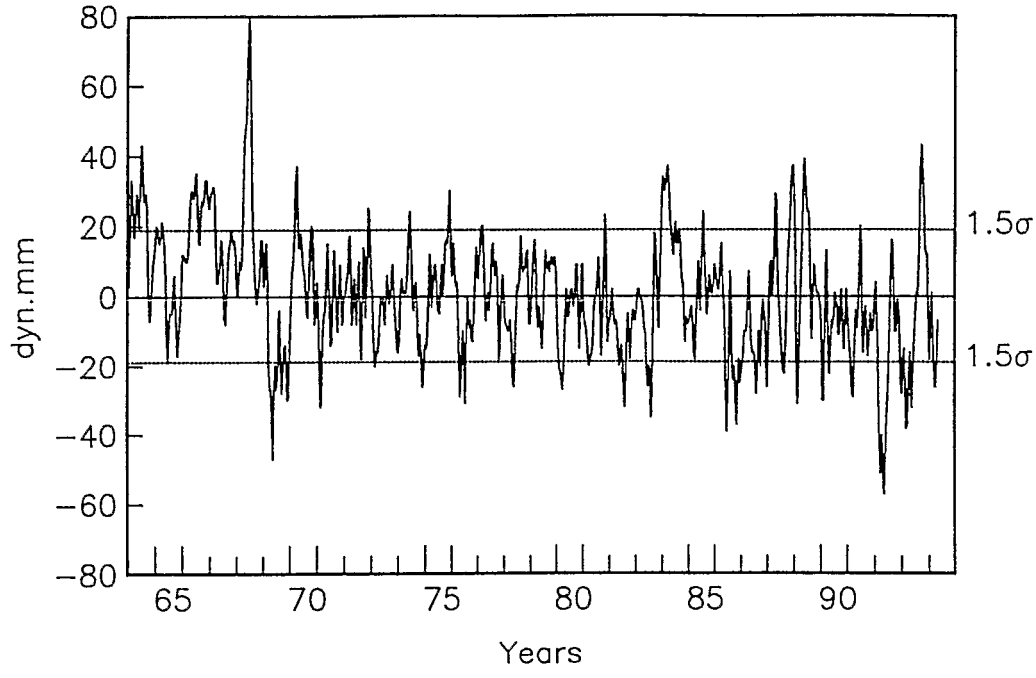

Figure 5

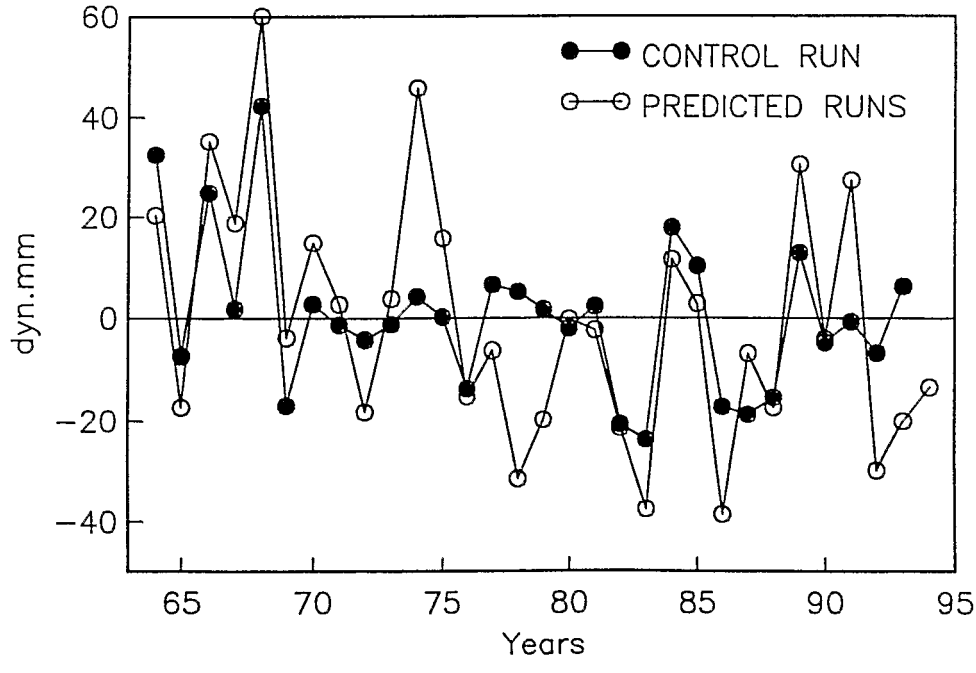

Figure 6

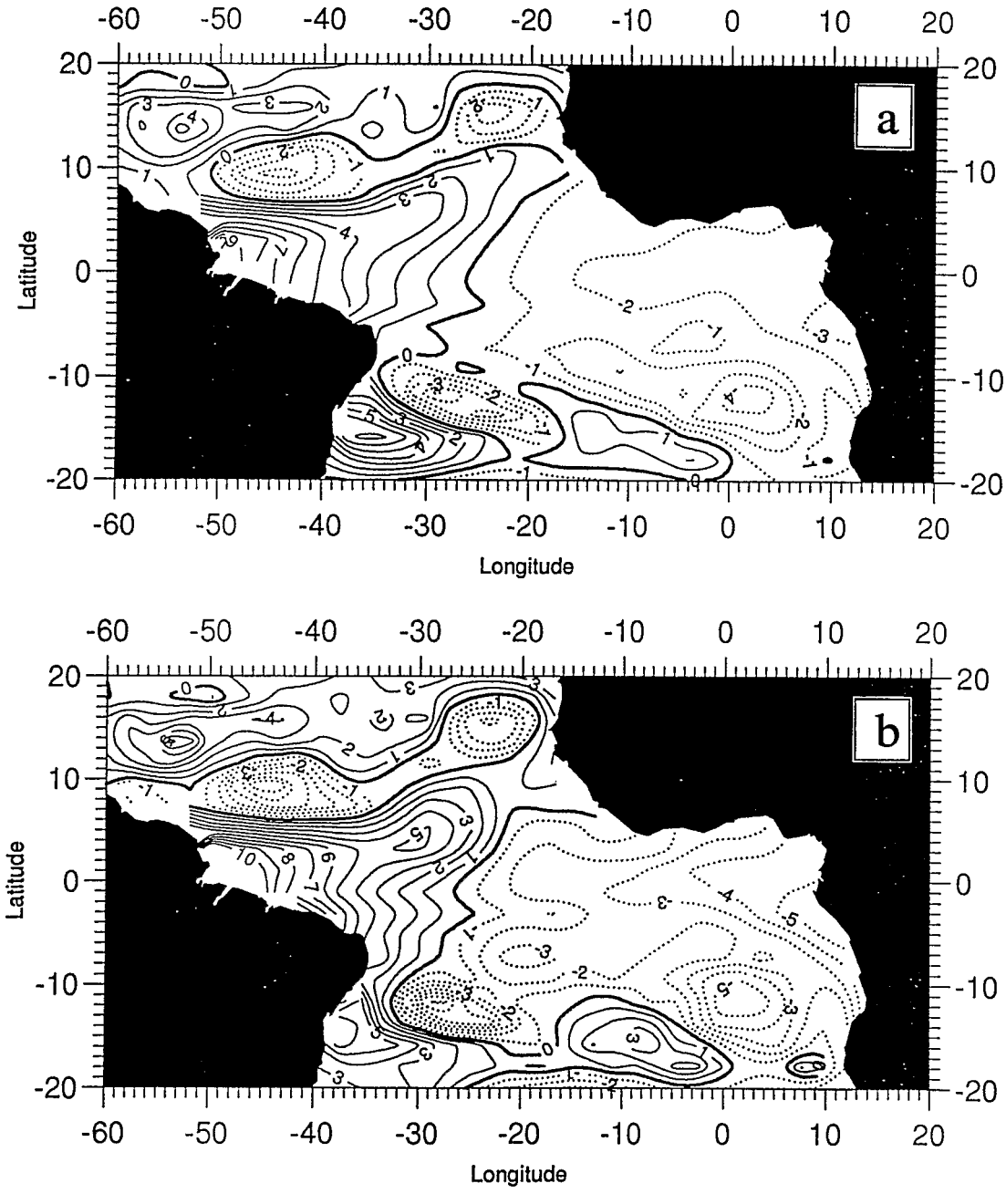

Figure 7

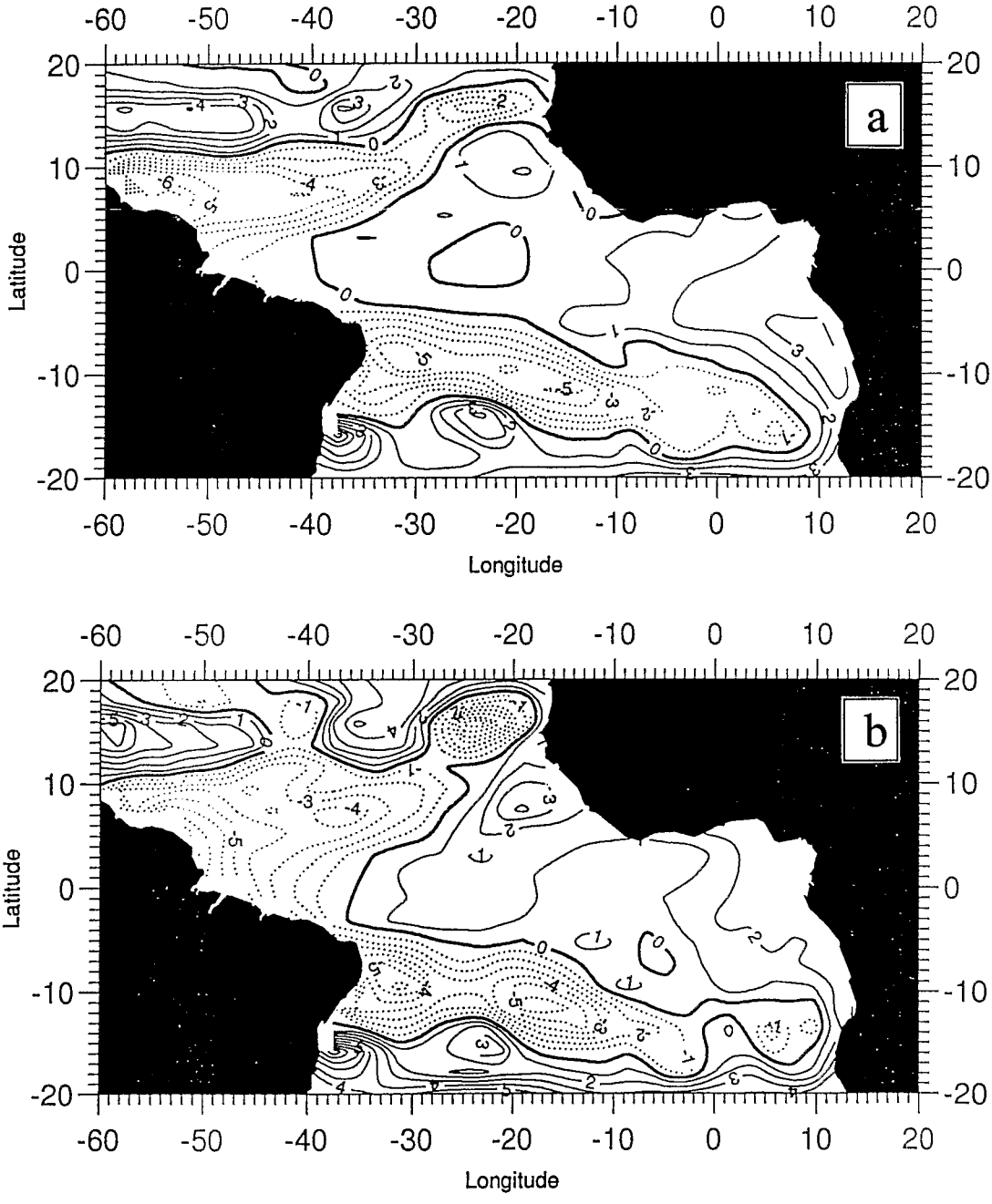

Figure 8

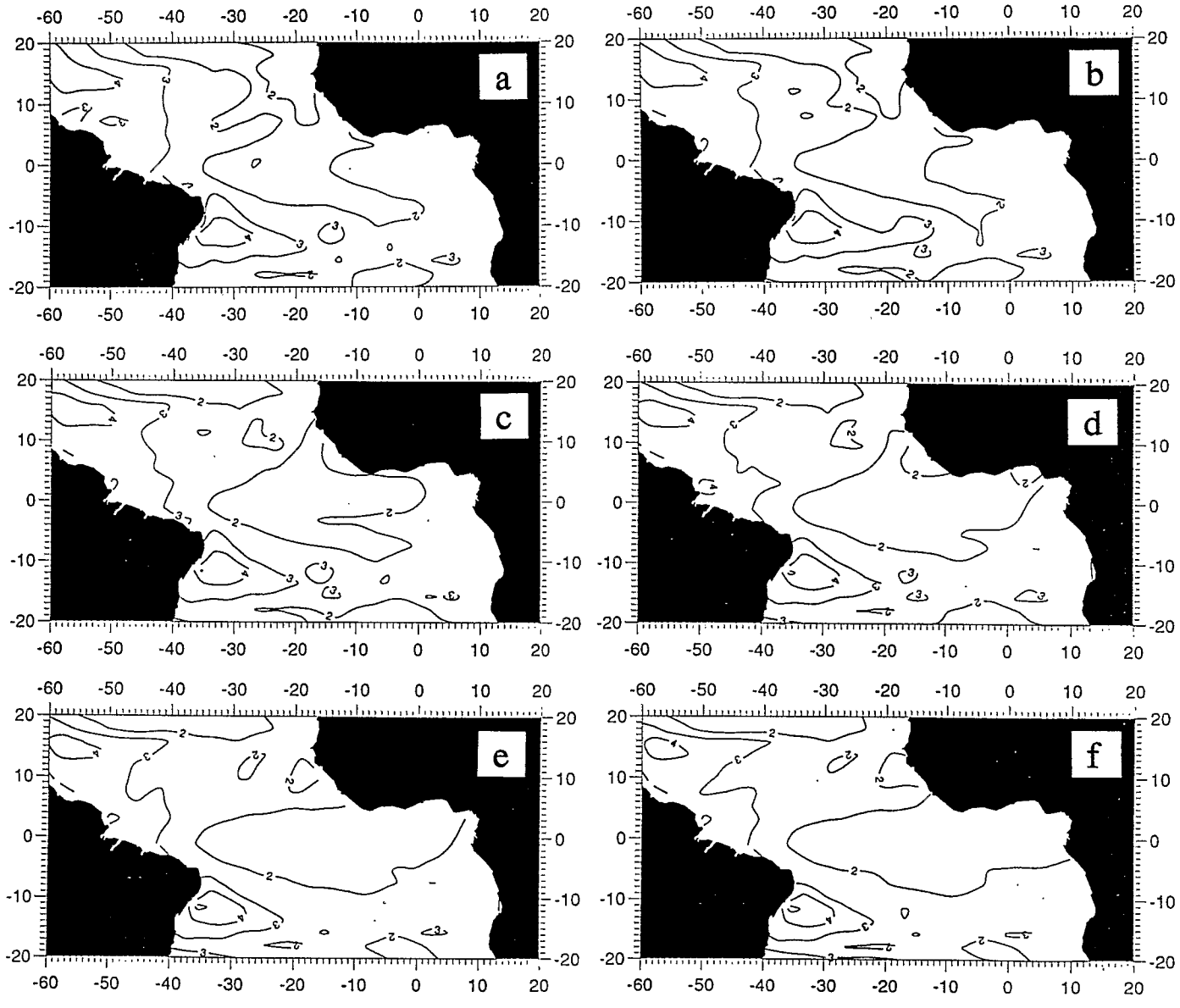

Figure 9

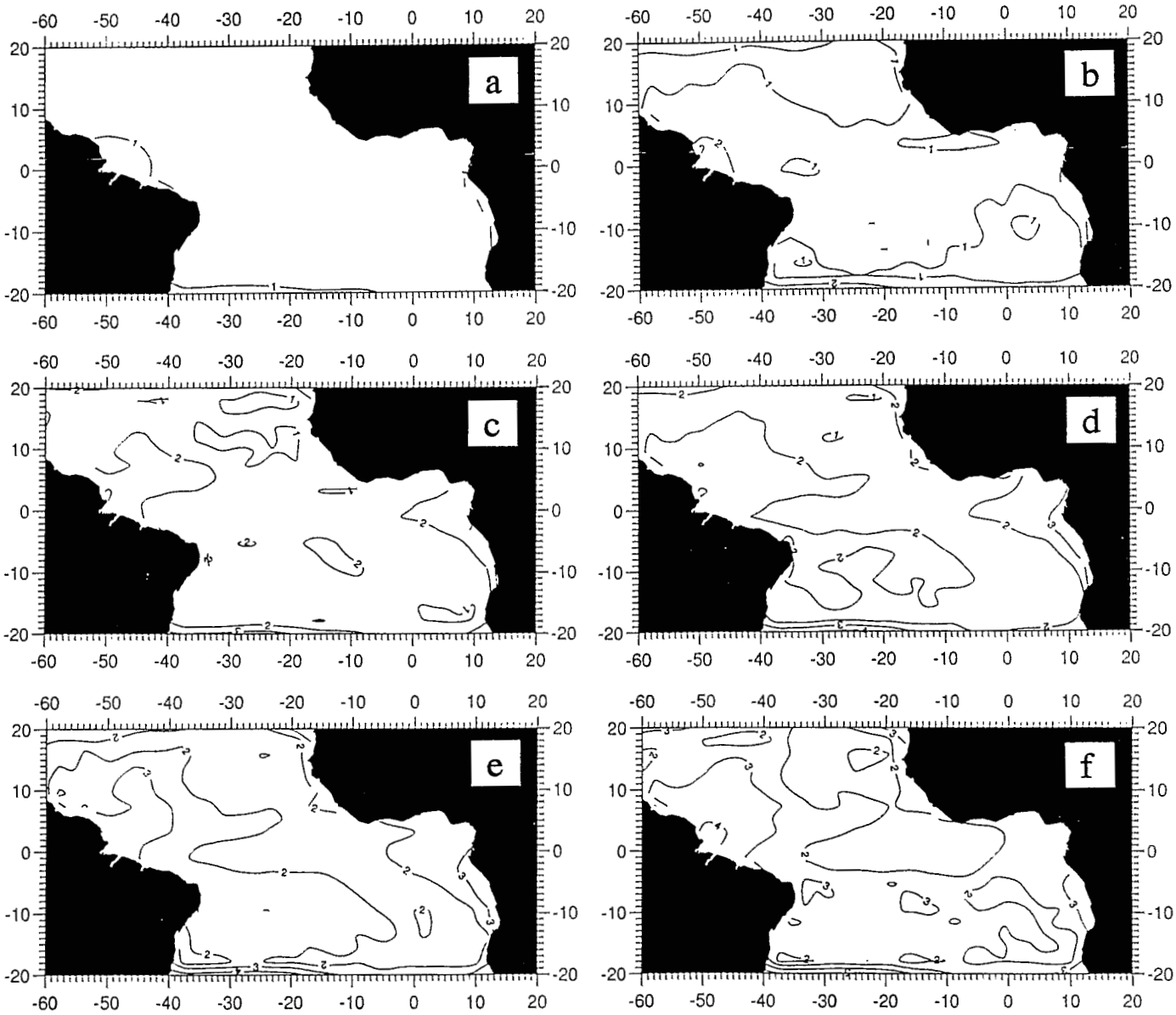

Figure 10

	JAN		FEB		MAR		APR		MAY		JUN		JUL		AUG		SEP		OCT		NOV		DEC	
1964	4	16	30	30	24	19	23	30	29	25	29	38	39	35	33	28	14	0	-9	-10	2	13	15	19
1965	25	26	22	20	17	15	13	11	8	-5	-18	-18	-5	-3	5	4	11	2	-12	-18	-18	-15	-2	13
1966	15	15	14	13	14	19	25	28	30	30	33	33	27	14	8	16	24	23	27	35	33	28	29	32
1967	28	26	27	28	21	10	3	1	5	10	11	7	4	2	2	6	10	14	18	18	17	16	13	4
1968	-2	1	10	13	12	28	44	48	51	63	75	70	49	30	13	1	-3	-6	-8	-4	5	15	19	17
1969	11	11	11	3	-13	-23	-32	-43	-51	-36	-23	-30	-26	-9	-5	-14	-19	-22	-24	-20	-17	-21	-23	-16
1970	-4	3	6	19	35	42	36	22	12	8	6	10	11	7	1	-5	-4	6	18	21	11	-2	-6	-4
1971	-8	-18	-28	-25	-10	4	1	5	17	14	6	-6	-16	-14	-2	9	9	4	2	5	1	-15	-17	-7
1972	-4	3	14	21	13	1	-3	0	4	0	-4	4	14	7	5	2	9	8	-3	4	20	21	14	11
1973	-6	-24	-25	-16	-10	-12	-14	-10	-8	-3	2	-3	2	7	-2	-8	-5	3	9	5	-3	-9	-18	-23
1974	-20	-6	5	7	2	-3	-7	-1	10	20	20	8	-5	-6	2	6	-2	-15	-20	-16	-18	-27	-26	-13
1975	-9	-9	-4	3	1	-3	5	12	8	2	-5	-12	-9	3	10	5	6	14	14	13	21	29	25	14
1976	9	9	4	4	5	-1	-18	-31	-29	-23	-21	-25	-29	-16	-2	-6	-9	-5	-13	-20	-10	4	19	23
1977	16	15	18	19	15	5	-7	-10	-4	-2	-5	1	10	10	12	15	12	3	-8	-19	-18	-3	5	1
1978	-1	-2	-8	-15	-17	-14	-19	-24	-25	-26	-17	-1	4	9	17	11	3	4	5	8	16	12	0	-6
1979	-6	-3	5	14	12	-1	-12	-11	-9	-17	-22	-15	-3	5	9	12	13	10	6	0	-2	5	14	11
1980	-3	-15	-23	-26	-27	-25	-22	-16	-5	0	-6	-8	-4	-5	-5	-1	4	13	16	-1	-18	-14	4	7
1981	1	0	-6	-19	-29	-25	-18	-18	-16	-8	5	11	6	7	9	8	-23	-16	3	19	18	1	-15	-14
1982	-14	-11	-3	-3	-14	-13	-8	-12	-20	-19	-12	-16	-29	-39	-40	-24	-8	-7	-15	-15	-3	-2	-12	-12
1983	-7	-5	-1	2	1	4	6	4	-3	-16	-29	-29	-24	-28	-24	-2	16	13	12	15	9	7	18	23
1984	24	34	40	39	36	32	23	21	19	15	26	31	21	15	21	19	8	7	6	-15	-24	-11	-6	-9
1985	-6	-3	-7	-11	-12	-16	-13	4	14	6	0	6	18	21	16	6	-5	-5	2	0	-3	-1	2	4
1986	7	10	8	6	10	15	10	-1	-7	-23	-38	-36	-25	-11	-5	-15	-25	-27	-31	-36	-28	-23	-25	-20
1987	-15	-18	-15	-6	-5	0	6	1	-13	-17	-15	-17	-19	-27	-31	-26	-30	-27	-2	11	1	-11	-20	-30
1988	-23	6	15	10	13	22	25	25	14	1	-7	-14	-23	-26	-21	-15	-1	16	23	30	36	35	31	27
1989	12	-14	-34	-35	-18	1	21	46	53	40	29	22	16	13	7	-1	3	13	13	5	-1	-2	-4	-3
1990	-7	-21	-26	-11	9	10	3	-4	-9	-9	-4	0	3	4	5	1	-4	1	1	-9	-13	-8	1	-1
1991	-8	-12	-18	-26	-30	-22	-12	-8	0	18	28	18	-6	-16	-11	-9	-17	-18	-7	2	2	-1	-5	-3
1992	0	-7	-19	-33	-48	-46	-42	-51	-55	-40	-27	-19	0	16	20	18	13	-2	-12	-6	2	-2	-18	-31
1993	-28	-21	-23	-28	-30	-18	-18	-31	-32	-20	-11	-3	1	0	14	36	43	38	26	14	12	12	-4	-18
1994	-10	1	-5	-17	-26	-26	-18	-7	-3	-9														

Table 1

	JAN		FEB		MAR		APR		MAY		JUN		JUL		AUG		SEP		OCT		NOV		DEC	
1964	4	16	30	30	24	19	23	30	29	25	24	22	19	18	18	17	.	.	.	.	.	.	.	.
1965	25	26	22	20	16	15	13	11	8	-3	-15	-20	-19	-18	-17	-13	.	.	.	.	.	.	.	.
1966	15	15	14	14	14	19	25	28	30	30	30	30	31	32	35	38	.	.	.	.	.	.	.	.
1967	28	26	27	28	21	10	3	1	5	10	14	15	16	18	19	18	.	.	.	.	.	.	.	.
1968	-3	1	10	13	12	28	44	48	51	63	72	69	62	55	48	41	.	.	.	.	.	.	.	.
1969	11	11	11	3	-13	-23	-32	-43	-51	-35	-16	-8	-1	4	5	1	.	.	.	.	.	.	.	.
1970	-4	3	6	19	35	42	36	22	12	7	3	6	10	11	11	13	.	.	.	.	.	.	.	.
1971	-8	-18	-28	-25	-10	4	1	5	17	18	16	15	10	3	-4	-7	.	.	.	.	.	.	.	.
1972	-4	3	14	21	13	1	-3	0	4	-4	-17	-22	-22	-25	-24	-19	.	.	.	.	.	.	.	.
1973	-6	-24	-25	-16	-10	-12	-14	-10	-8	-4	2	7	8	5	2	-1	.	.	.	.	.	.	.	.
1974	-20	-5	5	7	2	-3	-7	-1	10	25	39	47	49	48	47	44	.	.	.	.	.	.	.	.
1975	-9	-9	-4	3	1	-3	5	12	8	7	10	11	13	17	19	20	.	.	.	.	.	.	.	.
1976	9	8	4	4	5	-1	-18	-31	-29	-23	-24	-25	-23	-21	-20	-16	.	.	.	.	.	.	.	.
1977	16	15	18	19	14	4	-7	-10	-4	-2	-8	-8	-3	-2	-1	2	.	.	.	.	.	.	.	.
1978	-1	-2	-8	-15	-17	-14	-19	-25	-25	-31	-40	-41	-38	-36	-33	-29	.	.	.	.	.	.	.	.
1979	-6	-3	5	14	12	-1	-12	-11	-9	-15	-20	-22	-24	-27	-26	-23	.	.	.	.	.	.	.	.
1980	-3	-16	-23	-26	-27	-25	-22	-16	-5	0	-2	0	3	0	-2	-3	.	.	.	.	.	.	.	.
1981	1	0	-6	-19	-29	-25	-18	-18	-16	-9	-1	4	4	4	1	-3	.	.	.	.	.	.	.	.
1982	-14	-11	-3	-3	-14	-13	-8	-12	-20	-21	-21	-23	-25	-26	-27	-27	.	.	.	.	.	.	.	.
1983	-7	-5	-1	2	1	4	6	4	-3	-20	-40	-47	-47	-46	-42	-35	.	.	.	.	.	.	.	.
1984	24	34	40	39	36	32	23	21	19	14	18	22	19	17	19	20	.	.	.	.	.	.	.	.
1985	-6	-3	-7	-11	-12	-16	-13	4	14	6	1	3	3	1	2	3	.	.	.	.	.	.	.	.
1986	7	10	8	6	10	15	10	-1	-7	-22	-38	-41	-38	-39	-37	-32	.	.	.	.	.	.	.	.
1987	-16	-18	-16	-6	-4	0	6	1	-13	-15	-10	-7	-4	0	2	2	.	.	.	.	.	.	.	.
1988	-23	6	15	10	14	22	25	25	14	0	-8	-15	-23	-28	-28	-27	.	.	.	.	.	.	.	.
1989	12	-14	-34	-35	-18	1	21	46	53	44	42	41	36	29	24	19	.	.	.	.	.	.	.	.
1990	-8	-21	-26	-11	9	10	3	-4	-9	-7	0	2	3	4	3	0	.	.	.	.	.	.	.	.
1991	-8	-12	-18	-26	-30	-22	-12	-8	0	18	33	36	35	35	33	27	.	.	.	.	.	.	.	.
1992	0	-8	-19	-33	-48	-46	-42	-51	-55	-42	-34	-32	-27	-20	-18	-18	.	.	.	.	.	.	.	.
1993	-18	-15	-26	-38	-37	-23	-16	-28	-32	-20	-20	-22	-18	-20	-19	-21	.	.	.	.	.	.	.	.
1994	-10	1	-5	-17	-26	-26	-18	-7	-3	-9	-12	-8	-9	-13	-18	-20	.	.	.	.	.	.	.	.

Table 2

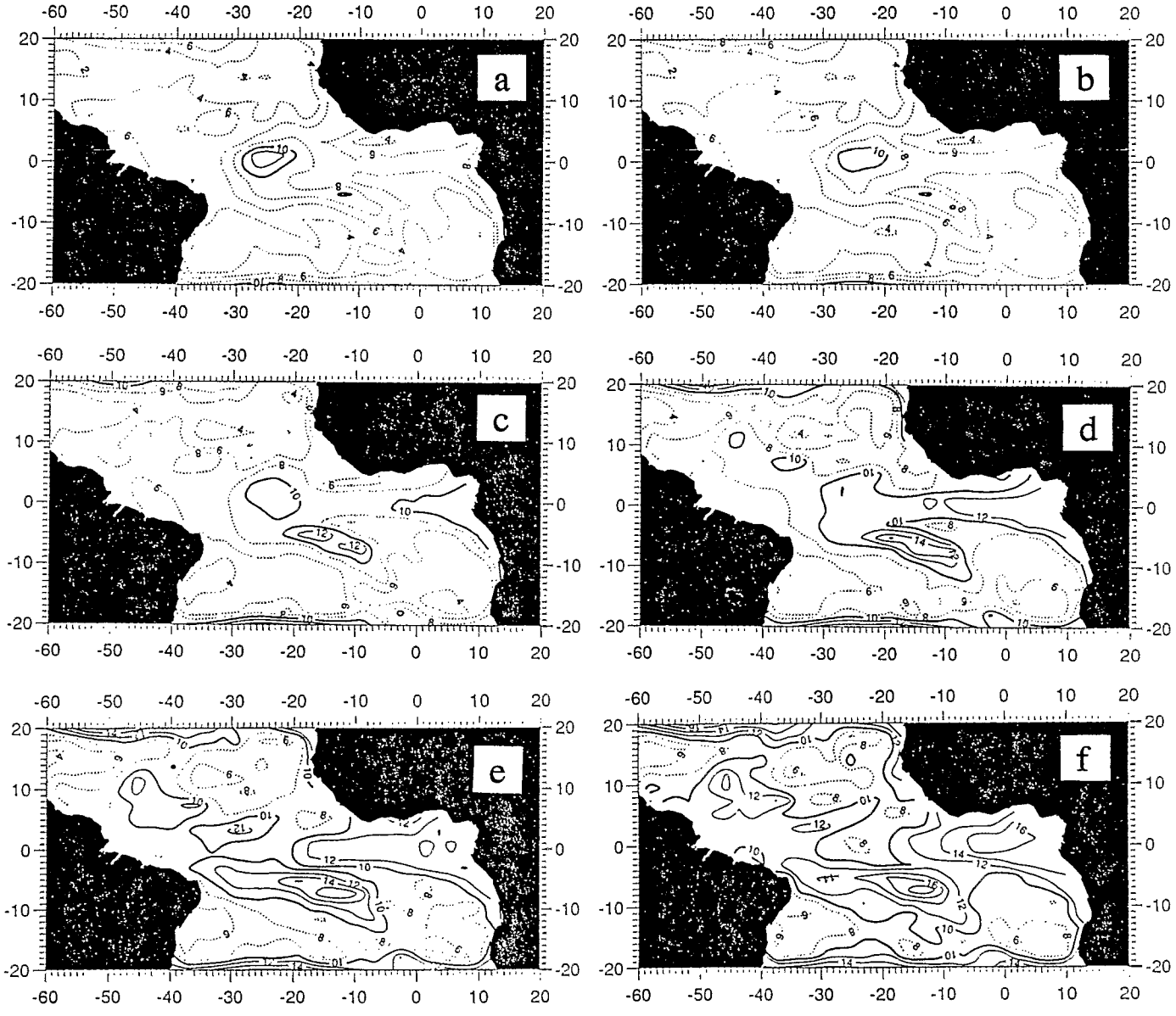

Figure 11